# Photoionization mass spectrometer with a microscope laser desorption source

Mattanjah S. de Vries, Donald J. Elloway, H. Russel Wendt, and Heinrich E. Hunziker
*IBM Almaden Research Center, 650 Harry Road, San Jose, California 95120-6099*

(Received 9 December 1991; accepted for publication 2 February 1992)

An apparatus is been described in which laser desorption, separate laser ionization, mass spectrometry, and microscopy are combined. An UV waveguide laser is focused on a sample, which is mounted on translation stages in vacuum. Desorbed neutral molecules are ionized above the surface by a second laser, and ions are extracted into a reflectron time of flight mass spectrometer. A spatial resolution of 1 $\mu$m is demonstrated, with a mass resolution of 2000 and a detection efficiency of $10^{-4}$.

## I. INTRODUCTION

The need for direct chemical analysis of heterogeneous objects with high spatial resolution today occurs in many areas of science and technology. Examples include plant and animal tissue, interstellar dust particles, microfossiles, and the microstructures of integrated electronic circuits, to name just a few. Techniques for spatially resolved *elemental* analysis are far advanced, available in commercial instruments (e.g., ESCA, SIMS, EDX, SAM), and have reached the stage of atom-by-atom reconstruction of an object.[1] By comparison, methods for direct *molecular* analysis with high spatial resolution are far behind, being fewer, less sensitive, and more cumbersome. The main obstacles are alteration of molecular structure during the processes of removal and detection, and the difficult task of molecular structure identification with minute amounts of material.

Apart from small-spot ESCA, which gives information about valence state and chemical bonding with some spatial resolution, the principal microanalytical, *in situ* techniques providing molecular information are SIMS[2-4] and the laser microprobe.[5-10] In their original form both techniques combined removal and ionization of the molecular material in a single step (ion or laser pulse), the analysis being done by mass spectrometry. More recently both techniques have been augmented by a post-ionization step to separately optimize conditions for neutral material removal and for ionization.[11-14] This separation provides higher overall sensitivity and more easily interpretable results.[15-21]

Ideally post-ionization of neutral molecules can be carried out by resonance enhanced multiphoton ionization (REMPI), providing additional selectivity. However, for complex molecules this approach requires combination with jet cooling.[21] No implementation of this variant has been described which permits high spatial resolution.

This article describes an implementation of two-step laser mass spectrometry (L2M) for high spatial resolution, in a new configuration. Odom *et al.* have reported the conversion of a commercial laser microprobe instrument for post-ionization.[14] Concurrent with this work a similar instrument was built by Zare and coworkers at Stanford.[22] Our instrument uses UV (248 nm) pulses for material removal, while the Stanford instrument uses a CO2 laser (10.6 $\mu$m). The trade-off is spatial resolution versus the risk of photochemical processes. In the following sections we describe our L2M microscope in detail and then give some examples of its performance.

## II. APPARATUS

### A. Overview

A schematic layout of the L2M microscope is shown in Fig. 1. A reflective lens with Cassegrainian optics is positioned inside a high vacuum chamber. It serves double duty for focusing a pulsed KrF desorption laser beam and as objective for a visual microscope. The laser beam is folded into the microscope by a beamsplitter. Details of the optics are described in Sec. II B below. Samples are introduced into the vacuum chamber by a special loadlock arrangement; once positioned under the lens, the sample is manipulated by *XYZ* stages, driven by piezo inchworm motors. The micropositioning, which is entirely computer controlled, is further detailed in Sec. II C. Desorbed molecules are laser ionized by either 266-nm radiation from a quadrupled Nd:YAG laser or 193-nm pulses from an ArF laser. The ions are extracted and focused into a reflectron TOF mass spectrometer. Special ion optics is required, as explained in Sec. II D. The vacuum chamber pressure is about $10^{-7}$ Torr. More important than the absolute pressure is the cleanliness, i.e., the partial pressure at the mass of the organic molecules to be detected. For this reason no oil diffusion pumps are used, but rather turbomolecular pumps, sorption pumps, and a LN2 cold trap. (As will be discussed below, the background signal is also minimized because it is discriminated against by the ion optics). A block diagram is given in Fig. 2 to show the timing logic of the experiments.

### B. Light optics

The heart of the light optics is a reflective objective, which was chosen for two reasons: (1) Reflective optics are achromatic. This makes it possible to use one lens, both as a visible light microscope objective and to focus UV laser light, with identical focal distances for both applications. The objective is adjusted for infinity so that the laser

 0034-6748/92/063321-05$02.00  

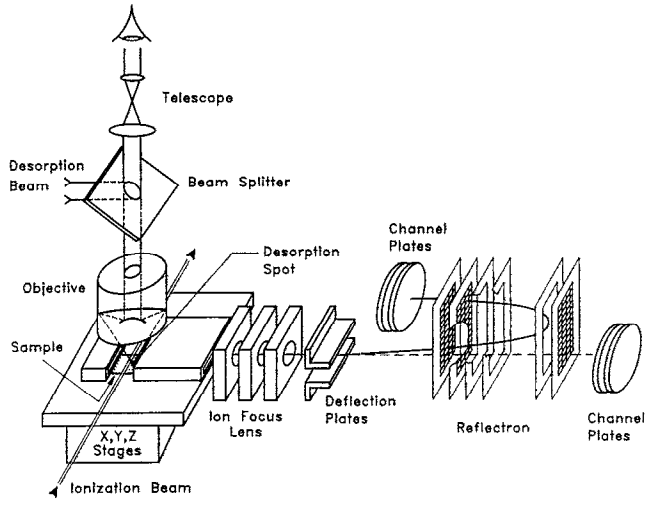


FIG. 1. Schematic layout of laser desorption mass spectrometer microscope. For the discussion in the text, the $z$ axis is taken vertically along the direction of the light optics; the $x$ axis is along the direction of the time of flight, to the right in the figure.

beam can be folded in with a beamsplitter. (2) A large numerical aperture can be achieved while maintaining a relatively large working distance of 8 mm. The former is important in order to achieve a minimum diffraction limited spot size, the latter is important to allow room for ion extraction. This type of objective is available from an increasing number of optical companies because of its usefulness in applications such as laser micromachining. Our lens is coated with $MgF_2$, and protected from desorbed debris by a disposable fused silica cover. The minimum spot size also depends on the wavelength and the beam quality of the desorption laser. An UV waveguide laser is used (Potomac Photonics), operating at KrF, 248 nm. The maximum pulse energy is 10 $\mu$J and 50% of the output is in TEM00 mode. Pulse duration is 50 $\mu$s. With this arrangement a spot size of 1 $\mu$m is obtained. Another advantage of this type of desorption laser is its pulse to pulse stability. This is important because laser desorption, unless it is complete, is a very steep function of laser fluence.

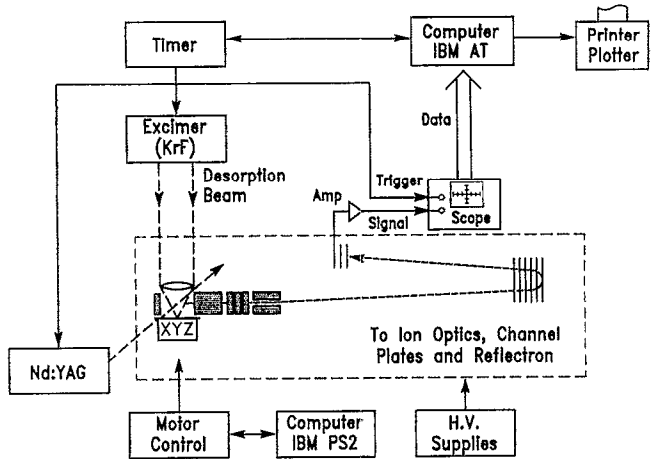


FIG. 2. Block diagram of laser desorption mass spectrometer microscope.

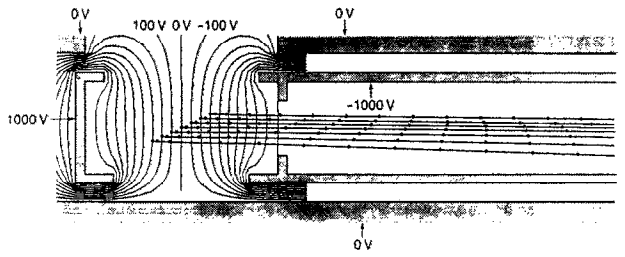


FIG. 3. Schematic view of extraction ion optics in the $z$-$x$ plane. Electrodes are indicated in gray. The distance between the top and bottom ground potential surface (lens cover and sample respectively) is 8 mm. The drawing is to scale. Equipotential contours are given with 100-V intervals. Heavier lines show ion trajectories for mass 40 ions starting at different points. Flight times are shown by dots at 25-ns intervals.

### C. Positioning

The sample is placed on $XYZ$ translation stages, which are driven by piezo inchworm motors (Burley). Feedback is provided for closed loop control by linear magnetic encoders (SONY). The circuitry is interfaced to a PS/2 computer by an IEEE bus. The arrangement allows for travel over a distance of more than 2.5 cm, with repeatability and step sizes of less than 1 $\mu$m. The sample introduction system is an integral part of the design. A sample holder is moved in the vacuum chamber along a rail mechanism. When positioned under the microscope, the sample holder is lifted from its carrier by the $Z$ stage, which is also used for focusing. When in the loadlock position, the sample holder is lifted from the carrier and pushed against an O ring surrounding the loadlock opening, for easy access. In a typical experimental sequence data are taken at a number of preprogrammed positions. At each point the computer program integrates preset peaks in the time of flight spectra, thus accumulating maps of a number of selected masses as a function of position.

### D. Ion optics

Very severe constraints exist for the design of the ion extraction optics in this setup. These constraints are imposed by the choice to first of all optimize the optical resolution. For this purpose the optical axis is taken normal to the sample surface (the $z$ direction) while the ions are extracted parallel to the sample surface (the $x$ direction). This makes it difficult to generate a homogeneous electric field, to serve as a good source for the time of flight mass spectrometer, because only 8 mm working distance is available between the optical lens and the sample surface. Thus it is necessary to take into account the potentials of the environment, in particular those of the sample and the lens. In order to be able to keep those surfaces at ground potential, a configuration was chosen as shown in Fig. 3.

Photoions are formed at a point halfway between the sample and the optical lens cover. This point is 4 mm above the sample. Figure 3 shows equipotential contours of the field created with the repeller electrode at + 1 kV and the extractor grid at − 1 kV. The contours are calculated with the SIMION program.[23] The ions are formed near the

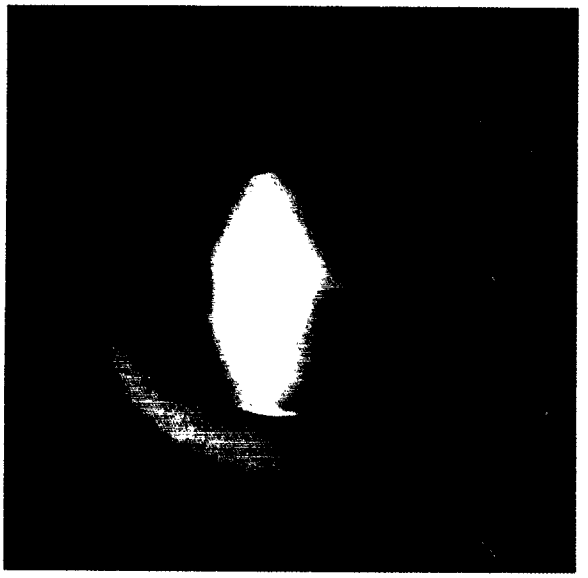

FIG. 4. Picture from phosphor screen detector behind reflector.

inflection point at approximately ground potential. Also shown in Fig. 3 are some ion trajectories. There are two characteristics of the ion trajectories that need to be optimized: (1) spatial focusing is important in order to achieve optimum collection efficiency and transmission, and (2) time focusing is required in order to achieve optimum TOF resolution.

This specific ion source configuration produces trajectories that are either focused or dispersed, depending on whether they start at the lower or higher voltage side, respectively, of the inflection point in the potential. Note that the actual position of the inflection point can be adjusted by changing the relative voltages on the electrodes. The trajectories will tend to go up or down in the $z$ direction, depending on where the starting points are along the $z$ axis. The velocity in the $z$ direction depends also on the initial velocity of desorbed molecules normal to the sample surface. In order to correct for these effects and to aim as many ions as possible towards the channel plate detector, the ion source is followed by an einzel lens and by deflection plates. For diagnostic purposes, a second channel plate detector with a phosphor screen is positioned behind the reflector. Figure 4 shows a picture taken from this phosphor screen, with the reflector voltages at flight tube potential. Coronene molecules were desorbed from copper and postionized with 266 nm. The blur in the $z$ direction is the result of the initial velocities of the desorbed molecules along that coordinate. Their velocity distribution differs from that of background molecules, requiring different voltages on the deflection plates to optimize the signal. This helps to discriminate against background ions. The final detector is mounted on a separate flange, and can be exchanged for one with a phosphor screen, permitting further visual observation of the alignment.

High resolution in time-of-flight mass spectrometry is achieved by making the flight time as insensitive as possible to variations of starting position and initial velocity of the ions. For a gas phase laser ionization source its width in the flight direction is the principal, limiting factor. The simplest and probably best way to deal with this is to form the ions in a high-field extraction region, from which they exit into field-free space after traveling a mean distance $s$.[24] This configuration has a fixed, geometric "space focus" at distance 2s from the exit grid, where ions which started at different positions arrive at the same time but with different velocities.[25] This space focus is then used as the starting position of a reflectron, a device which compensates for variations of ion velocity.[26,27] There is a residual spread in starting time at the space focus caused by the variation of initial ion velocity, $\Delta v_0$, in the ionization volume. This spread is known as the "turnaround time" and can be shown to be $\Delta T = -\Delta v_0 m/Ee$ at the space focus. Thus $E$, the extraction field, is made as large as possible to minimize $\Delta T$. In our instrument $E$ is 2 kV/cm and $\Delta T$ is comparable to the duration of the ionizing laser pulse for a $m = 100$ amu ion. Since the properties discussed are strictly valid for small variations only, there is a trade-off between sensitivity and resolution: A large ionization beam diameter will increase sensitivity by producing more ions (at constant power density), but it will decrease resolution.

Our reflectron was built by R. Jordan & Co. as a prototype. It has a liner to keep the entire flight path at the potential of the negative extraction electrode, which allows the sample to be at ground potential. The channel plate detector can be used in a post-acceleration mode for detection of higher masses.

Absolute detection efficiency—the number of ions detected per neutral molecule removed—depends on geometric and kinematic (velocity distribution) factors, and on ionization efficiency. The first two factors are of the order $10^{-2}$ and $10^{-1}$, respectively, while ionization efficiency is at best $10^{-1}$ for a two-photon ionization process if excessive fragmentation of the molecular ion is to be avoided. Overall detection efficiency is thus estimated to be about $10^{-4}$, less for inefficiently ionized molecules.

## III. RESULTS

Figure 5 shows part of a mass spectrum obtained for a sample of $C_{60}$ with natural $^{13}C$ abundance (1.1%). The mass peaks at 720, 721, 722, and 723 thus represent 51.5, 34.4, 11.3, and 2.4% of all $C_{60}$ molecules. They are completely resolved but stand on a background which is due to delayed ionization of superexcited $C_{60}$ molecules. The mass resolution in this spectrum is about 2000, and the peak width of 37 ns is about twice the pulse width of the ionizing laser.

The performance of the L2M microscope was tested with coronene in a number of different ways. A droplet of a benzene/coronene solution was placed on a polished silicon surface and the solvent was allowed to evaporate. Figure 6 shows the resulting pattern of coronene rings, each 1–4 $\mu$m wide. A single scan was made along the radius of the droplet, while monitoring the signal at mass 300, the parent mass of coronene. The resulting signal as a function of position is also shown in Fig. 6 on the same distance scale as the visual picture. Clearly, the mass 300 signal

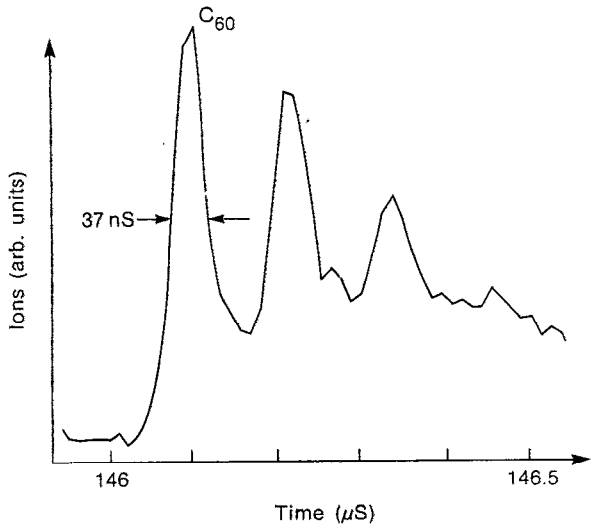


FIG. 5. Portion of mass spectrum of desorbed $C_{60}$, ionized at 193 nm. The natural isotope peaks are imposed on a background which is due to delayed ionization of superexcited molecules.

maps the spatial distribution of the coronene on the surface, demonstrating the spatial resolution.

In another test a stripe pattern of coronene was created by evaporation through a lithographic mask. The stripes were 150-$\mu$m wide and separated by 150 $\mu$m. The film thickness was 100 Å. The stripes were covered by a continuous 100-Å film of perylene. A scan was made at right angles to the stripes, while monitoring both the coronene mass (300 amu) and the perylene mass (252 amu). Figure 7 shows the ratio of the 300 and 252 amu signals. Use of the perylene signal as internal standard has eliminated a large portion of the shot-to-shot fluctuations which are otherwise present (compare for example with Fig. 6).

One important application is the identification of organic particles. Figure 8 shows a picture of a coronene

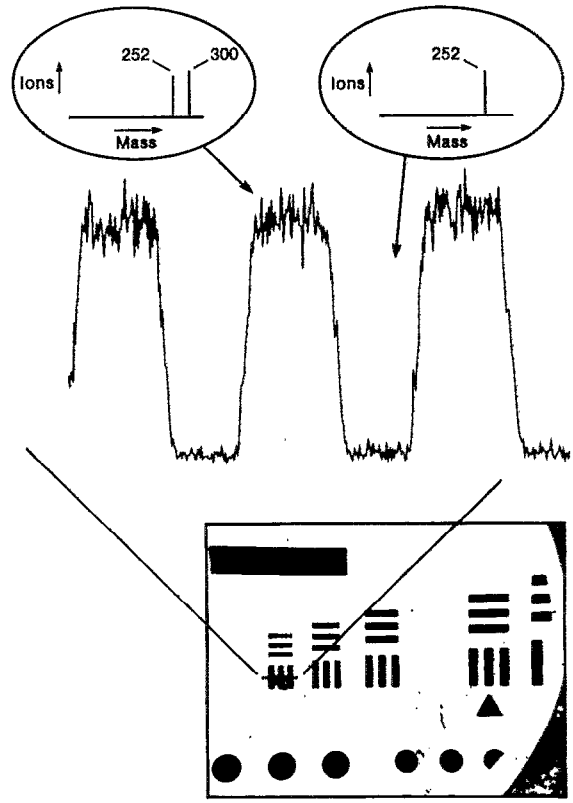


FIG. 7. Stripe pattern from evaporating coronene through a mask. The coronene is covered by a continuous perylene layer. The top part of the figure shows the ratio of the coronene and perylene signals obtained as a line scan is made through the stripes, which are 150-$\mu$m wide.


FIG. 6. Picture of a ring pattern resulting from evaporating a droplet of coronene solution on silicon. The rings are 1–4 $\mu$m wide. Superimposed on the picture is the signal obtained at mass 300 as a single line scan is made through the pattern.

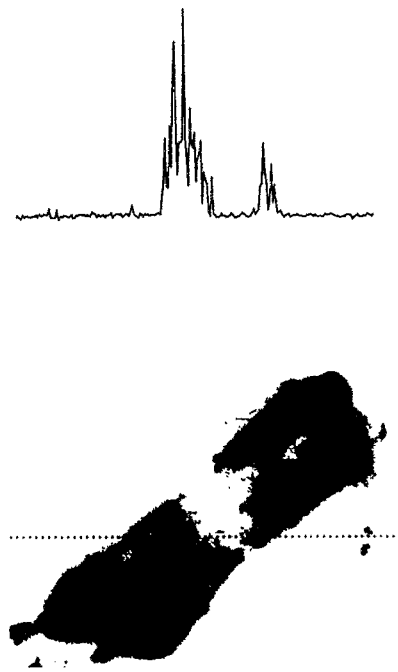

FIG. 8. Picture of a coronene particle, 100-$\mu$m long and 25-$\mu$m across. Top part shows mass 300 signal as a line scan is made along the direction indicated by the dotted line.

particle, made by atomizing coronene from a benzene solution. A scan was made through the particle along the direction indicated in the picture. Note that the picture was taken after the measurement, to show the small amount of material needed for the analysis. The mass 300 signal as a function of position is also shown in Fig. 8. The particle diameter was 25 $\mu$m. Because of the topography in the $z$ direction, the desorption laser was in focus only at the edges and the signal disappears in the center of the particle. It is possible in principle to map an object along the $z$ axis as well by adjusting the focus for maximum signal at every $XY$ position. The applications described here demonstrate the capability to detect neutral molecules with post-ionization and high spatial resolution. This approach opens the way to many applications in organic microanalysis.

## ACKNOWLEDGMENT

The authors thank Robert Mizrahi for mechanical design work.

[1] A. Cerezo, T. J. Godfrey, and G. D. W. Smith, Rev. Sci. Instrum. **59**, 862 (1988).
[2] A. Benninghoven, F. G. Ruedenauer, and H. W. Werner, *Secondary Ion Mass Spectrometry: Basic Concepts, Instrumental Aspects, Applications, and Trends* (Wiley, New York, 1987).
[3] D. Schuetzle, T. J. Prater, S. Kaberline, J. E. de Vries, A. Bayly, and P. Vohralik, Rev. Sci. Instrum. **60**, 53 (1989).
[4] J. L. Hunter, Jr., R. W. Linton, and D. P. Griffis, J. Vac. Sci. Technol. A **9**, 1622 (1990).
[5] F. Hillenkamp and E. Unsoeld, Appl. Phys. **8**, 341 (1975).
[6] R. Kaufman, F. Hillenkamp, and R. Wechsung, Med. Prog. Technol. **6**, 109 (1979).
[7] T. Dingle, B. W. Griffiths, J. C. Ruckman, and C. A. Evans, Jr., Microbeam Anal. **1982**, 365 (1982).
[8] D. M. Hercules, R. J. Day, K. Balasanmugam, T. A. Dang, and C. P. Li, Anal. Chem. A **54**, 280 (1982).
[9] A. W. Zbigniew and D. M. Hercules, Anal. Chem. **59**, 1819 (1987).
[10] J. T. Brenna and W. R. Creasy, Appl Spect. **45**, 80 (1991).
[11] N. Winograd, J. P. Baxter, and F. M. Kimock, Chem. Phys. Lett. **88**, 581 (1982).
[12] S. Mayo, T. B. Lucatorto, and G. G. Luther, Anal. Chem. **54**, 553 (1982).
[13] C. H. Becker and K. T. Gillen, Anal. Chem. **56**, 1671 (1984).
[14] R. W. Odom and B. Schueler, *Lasers and Mass Spectrometry,* edited by D. M. Lubman (Oxford University, Oxford, 1990), pp. 105–137.
[15] V. S. Antonov, S. E. Egorov, V. S. Letokov, and A. N. Shibanov, Chem. Phys. **85**, 349 (1984).
[16] H. von Weyssenhoff, H. L. Selze, and E. W. Schlag, Z. Naturforschung **40a**, 674 (1985).
[17] R. Tembreull and D. Lubman, Anal. Chem. **58**, 1299 (1986).
[18] F. Engelke, J. H. Hahn, W. Henke, and R. N. Zare, Anal. Chem. **59**, 909 (1987).
[19] B. Schueler and R. W. Odom, J. Appl. Phys. **61**, 4652 (1987).
[20] R. C. Estler, E. C. Apel, and N. S. Nogar, Int. J. Mass Spec. Ion Proc. **61**, 337 (1987).
[21] G. Meijer, M. S. de Vries, H. R. Wendt, and H. E. Hunziker, Appl. Phys. B **51**, 1871 (1990).
[22] L. J. Kovalenko, C. R. Maechling, S. J. Clemett, J. -M. Philippoz, R. N. Zare, and C. M. O'D. Alexander (to be published, 1992).
[23] D. A. Dahl and J. E. Delmore, Informal Report vol. EGG-CS-7233, (1986).
[24] R. B. Opsal, Dissertation, Indiana University, Diss. Abstr. Int. **47/02-B**, 604 (1985).
[25] W. C. Wiley and I. H. McLaren, Rev. Sci. Instrum. **26**, 1150 (1955).
[26] V. I. Karataev, B. A. Mamyrin, and D. V. Shmikk, Sov. Phys. -Tech. Phys. **16**, 1177 (1972).
[27] B. A. Mamyrin, V. I. Karataev, D. V. Shmikk, and V. A. Zagulin, Sov. Phys. JETP **37**, 45 (1973).